Pflugers Arch - Eur J Physiol (2002) 445:161–166
DOI 10.1007/s00424-002-0903-0

INSTRUMENTS AND TECHNIQUES

Stephen R. Besch · Thomas Suchyna · Frederick Sachs

High-speed pressure clamp

Received: 20 March 2002 / Accepted: 28 June 2002 / Published online: 9 August 2002

Abstract We built a high-speed, pneumatic pressure clamp to stimulate patch-clamped membranes mechanically. The key control element is a newly designed differential valve that uses a single, nickel-plated piezoelectric bending element to control both pressure and vacuum. To minimize response time, the valve body was designed with minimum dead volume. The result is improved response time and stability with a threefold decrease in actuation latency. Tight valve clearances minimize the steady-state air flow, permitting us to use small resonant-piston pumps to supply pressure and vacuum. To protect the valve from water contamination in the event of a broken pipette, an optical sensor detects water entering the valve and increases pressure rapidly to clear the system. The open-loop time constant for pressure is 2.5 ms for a 100-mmHg step, and the closed-loop settling time is 500–600 μs. Valve actuation latency is 120 μs. The system performance is illustrated for mechanically induced changes in patch capacitance.

Keywords Pressure clamp · Techniques · Stretch-activated channels · Mechanotransduction · Membrane capacitance

Introduction

The study of mechanosensitive ion channels has required the development of high-speed pressure stimuli to study relaxation processes. The first was a liquid-filled device that used a voice coil actuator [7]. This design had an adequately fast response (1–2 ms), but became unstable when air bubbles got into the tubing. Furthermore, filling and maintaining the system was difficult and messy. A much improved, fully pneumatic design was introduced by Hamill and McBride [2, 3, 4, 5]. This device used a pair of piezoelectric valves with a feedback control circuit. Although theoretically slower than the liquid-filled design, this pressure clamp could attain millisecond response times, and it resolved most of the stability issues that had plagued the liquid-filled clamp. However, achieving optimal performance with the pneumatic system was difficult in practice and valve failures were common.

The dynamic response of the McBride and Hamill clamp was dominated by the piezo valves (LFPA series, Lee, Essex, Conn., USA). They have a strong mechanical resonance at 1 kHz, and the feedback loop must be slowed to prevent mechanical ringing of the valve on step changes in pressure. Secondly, the internal volume of the valves and interconnecting tubing was substantial, further slowing the response time. Finally, the location of the pressure sensor far from the valve orifices introduced a delay in the response of pressure to a command voltage. This latency is impossible to compensate, and required further slowing of the closed-loop response time to make the feedback loop unconditionally stable over the ±200 mmHg pressure range. Valve failures stemmed from the need to maintain a high continuous bias voltage and from saline being drawn into the valve and short-circuiting the piezo element [6]. This occurred when a patch electrode broke or suction was applied when the pipette was removed from the holder.

In the new design we have sped up the intrinsic valve response time by (1) supporting the piezo bimorph at both ends, approximately doubling the resonant frequency of the single-ended support; (2) minimizing dead volume, and (3) placing the pressure sensor on the valve body. We have virtually eliminated valve breakdown by using piezo elements that don't require a static bias voltage (160–190 V) and constructing the valve so that zero pressure requires zero voltage. To eliminate the saline-induced short circuiting, we incorporated a "cough" function that is triggered when water is detected in the output line.

S.R. Besch (✉) · T. Suchyna · F. Sachs
Center for Single Molecule Biophysics, 320 Cary Hall,
SUNY at Buffalo, Buffalo, NY 14214, USA
e-mail: sbesch@acsu.buffalo.edu
Tel.: +1-716-8293289 ext. 106
Fax: +1-716-8292569

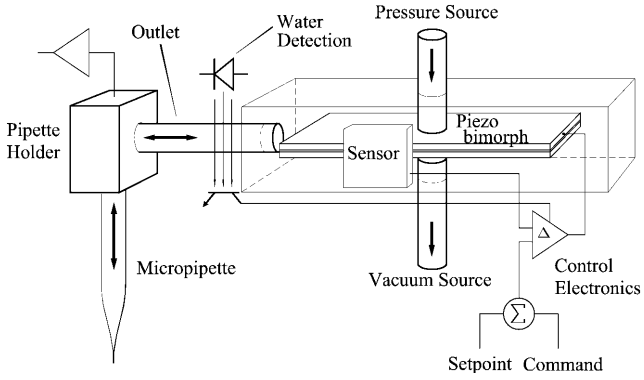

Fig. 1 Schematic of the pressure clamp system showing the main components. The micropipette is connected with 10 cm of silicone rubber tubing

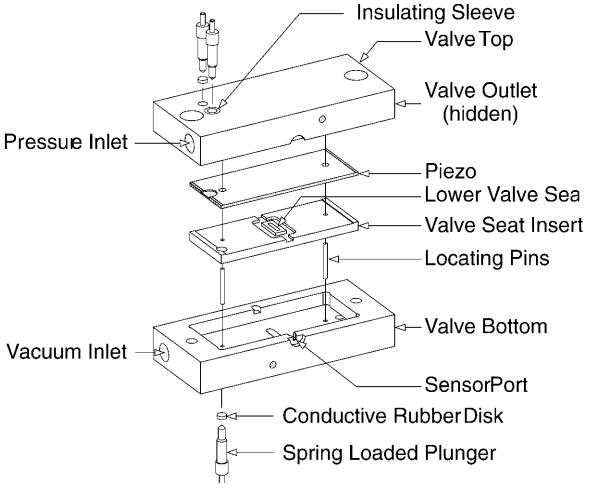

Fig. 2 Exploded view of valve

Methods and materials

A schematic of the pressure clamp system is shown in Fig. 1. It consists of four basic components: the piezoelectric valve, the control electronics and pressure sensor, the water detector, and the pressure/vacuum source. The valve, pressure sensor and water detector are enclosed in a small aluminum housing to protect the sensor electronics and provide electrostatic shielding.

The piezoelectric valve

The finished valve is 45 mm long, 19 mm wide, and 13 mm high, and is split physically into a top and bottom half. An exploded view of the valve is shown in Fig. 2. The valve's pressure seat is machined directly into the top. It is not visible in Fig. 2, but is structurally identical to the vacuum seat, which is shown. The vacuum seat is milled into a separate piece of aluminum that fits in a cavity in the bottom, and is supported on two cone-point set screws (not shown) that allow trimming position of the insert to match the thickness of the bimorph. The bimorph is sandwiched between the valve seats and supported only at its ends. The bimorph bends toward or away from the valve seats when voltage is applied, producing a proportional valve action. When the valve is assembled, a pair of locating pins maintains the internal alignment of the valve seats to the bimorph. It is important that the bimorph be allowed to "float" between the two valve seats.

The clearance between the bimorph and the seats is set by four short "gauge" wires glued to the bimorph. During assembly, the cone-point set screws are adjusted until the gauge wires just touch their respective support surfaces. The space under the insert is filled with silicone sealant. The mating surfaces of the top and bottom halves of the valve are honed flat and require no sealant. The valve seats are small rectangular pedestals on the inner surfaces of the valve body and insert. Slots milled into these pedestals (0.8×4 mm) communicate with drilled passages that connect to the pressure and vacuum sources. Clearance of 1.59 mm around the pedestals provides a low resistance pathway to the valve outlet.

The bimorph is a 12.7×31.75-mm element manufactured by Piezo Systems (Cambridge, Mass., USA). It consists of two nickel-plated piezo layers bonded to a non-metallic center shim. Control voltage is applied to the center shim and the outer nickel-plated layers are grounded. We removed a small portion of one of the piezo layers to expose the center shim for electrical contact. Locating holes were drilled through the element at either end. Electrical contact to the bimorph comes through three gold-plated spring contacts installed in the valve body. One of these is insulated with an epoxy sleeve and makes contact with the center shim. The remaining two are connected electrically to the metal body of the valve and ground the top and bottom surface electrodes. Arcing at the ground contacts was a problem. To obtain a reliable contact between these pins and the nickel plating, conductive silicone rubber disks (Zoflex CD45, Xilor, Knoxville, Tenn., USA) are placed under the tips of the pins and glued to the piezo using a conductive silicone rubber adhesive (Xilor).

Inherent in this design is an idling air flow through the valve at zero pressure. The amount of this flow is controlled by the spacing between the piezo and the valve seats and is set by means of the gauge wires. These are cemented to the ends of the bimorph using UV-curable epoxy. The proper size of the gauge wires was determined empirically and reflects the fact that the density of air is different under vacuum and pressure. The pressure seat spacing must be smaller than the vacuum seat spacing to achieve zero pressure with an unbiased piezo. The greater opposing force applied to the pressure side of the piezo also decreases the maximum distance that the piezo can move towards the pressure seat. A narrower gap on the pressure side of the piezo compensates for this effect and helps to balance the response time for vacuum vs. pressure. The optimal gauge wires were ~0.03 mm for pressure and 0.056 mm for vacuum. With these gaps, the idling flow was ~1 l/m with a supply of ~±300 mmHg. The valve's physical characteristics are summarized in Table 1.

Table 1 Summary of valve characteristics

Internal valve volume	235 µl
Vacuum seat gap	0.03 mm
Pressure seat gap	0.056 mm
Valve zero pressure idle flow	1 l/m
Piezo driving voltage range	±90 V
Piezo source driving resistance	100 Ω
Piezo capacitance	0.058 µF
Piezo response time	400 µs
Piezo resonant frequency	1.41 kHz
Open loop time constant (100-mmHg step)	2.53±0.02 ms
Valve activation delay	120 µs

Water detector

The water detector is an optical device that exploits the difference in the refractive index between air and water (Fig. 3). Polyethylene tubing (1.0 mm O.D.) is cemented between a photodiode/photodetector pair (OP299/OP535A, Optek, Carrollton, Tex., USA) machined to permit the emitter and detector to be positioned close

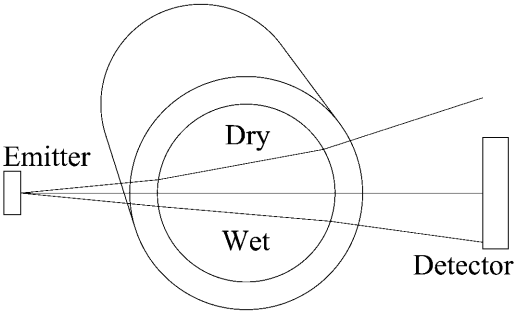

Fig. 3 Water detector. Water in the tube focuses light on the detector, increasing its output

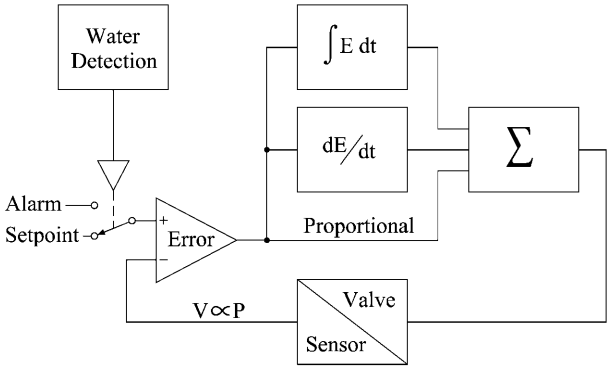

Fig. 4 Electronics block diagram. Output pressure is compared with the set-point and the error is used to drive the valve in a negative feedback loop. The set-point is derived from an input command voltage. The water detector replaces the set-point with a positive command voltage when water enters the valve inlet

to the tubing. The tubing acts as a cylindrical lens that shortens its focal length when water enters the tube and increases the amount of light reaching the detector. The detector produces an output signal that is used to switch the valve to a positive pressure, preventing water and salt from entering the valve.

Control electronics

A block diagram of the valve controller is shown in Fig. 4. It consists of a high-voltage driver-amplifier in a proportional-integral-differential feedback loop. The error voltage drives a high-voltage output amplifier (PA42, Apex Microtechnology, Tucson, Ariz., USA) operating at a gain of 7. The 3-dB roll-off of the output amplifier and preamp stages are nominally set to 500 Hz. This is necessary to suppress mechanical ringing of the piezo element in the valve.

Pressure and vacuum sources

A pair of reciprocating resonant piston pumps (pressure: VP0125; vacuum: VP0140; Medo USA, Hanover Park, Il., USA) were used to generate pressure and vacuum. Separate pumps were required for efficient delivery of both pressure and vacuum. In addition, 250-ml buffering canisters were placed in the pressure and vacuum lines to filter the 60-Hz pressure fluctuations of the pump.

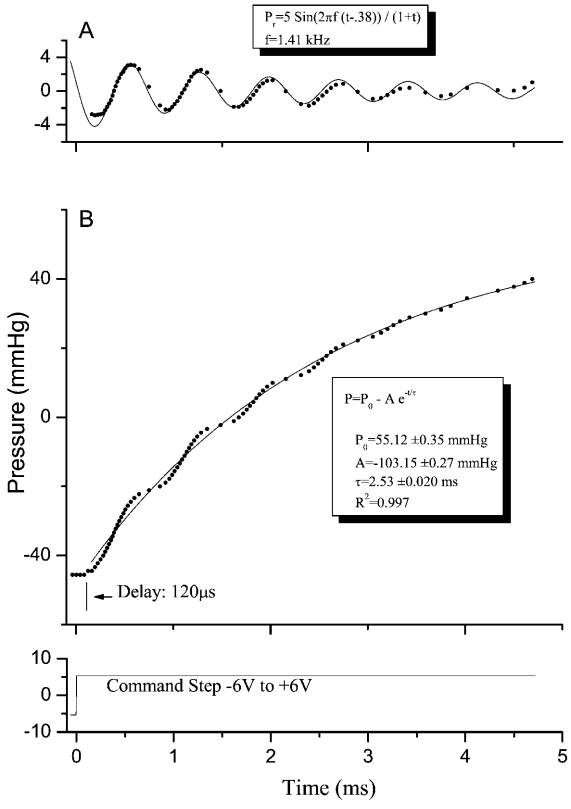

Fig. 5A, B Open-loop responses. The ringing of the piezo (**A**) was obtained by subtracting an exponential fit to the rise time (**B**) from the total

Results

Figure 5 illustrates the open-loop response of the valve to a step command. Pressure was measured with the valve-mounted transducer and the valve output was terminated with a 30-cm length of 1.6 mm ID PVC tubing. The result is shown in Fig. 5B.

The latency from the initial application of the command voltage to the change in output pressure was 120 μs. A single exponential fit to the rising phase of the pressure transition provided an estimate of the time constant as 2.5 ms. This is dominated by the time taken to fill/empty the valve with air. The published response time of the piezo element in a simple cantilever configuration is 400 μs, and that of the pressure sensor is <100 μs. The electrical charging time of the piezo capacitance is only 5.8 μs and can be ignored.

In open loop, the rise time of the driving step is sufficiently fast to cause the piezo to ring at its characteristic frequency of 1.4 kHz (Fig. 5A). Figure 6 shows the closed loop responses of the valve for three different pressure step amplitudes. This data is summarized in Table 2. Response times are given as the 0–90% values and as the time for the pressure to return to the set-point after an initial overshoot. The longer rise time of the larger amplitude steps is characteristic of closed-loop responses since the valve is saturated. Smaller steps are in

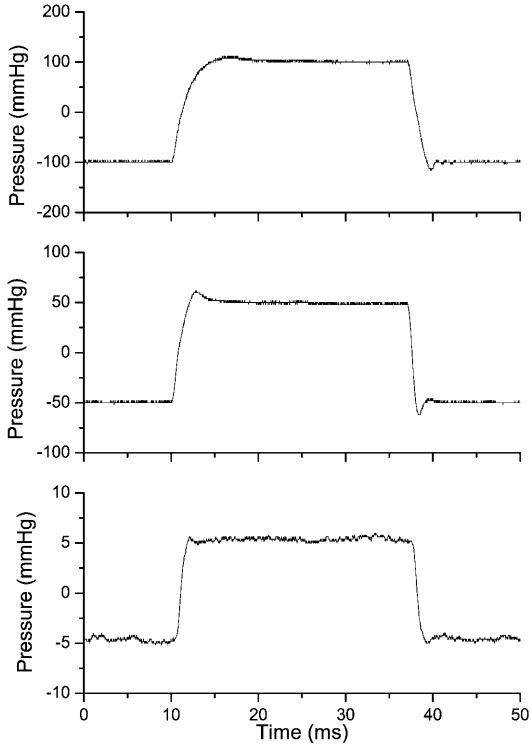

Fig. 6 Closed-loop responses. Step sizes were chosen to illustrate the response over the operating range of the pressure clamp. Timing details are given in Table 2

Table 2 Closed loop rise and fall times

Step Size	Rise times		Fall times	
	0–90%	Settling	0–90%	Settling
200 mmHg	3.0 ms	5.3 ms	1.9 ms	3.4 ms
100 mmHg	1.5 ms	4.0 ms	900 µs	3.0 ms
20 mmHg	880 µs	2.0 ms	880 µs	2.0 ms

the proportional domain and consequently more rapid. The rise time is slower than the fall time, probably because the vacuum seat spacing is larger than the pressure spacing.

The pressure response measured at the valve is nearly independent of the connecting tubing. However, the size and length of the tubing will affect the pressure waveform at the end of the tube. We measured the effect of the tubing material, length and diameter on the response characteristic with a second transducer at the end of the tubing, and the results are summarized in Table 3. The tubing had two main effects: an increase in latency proportional to length, and a slowing of the response time for large volume tubes. The tubing elasticity also had an influence that was more difficult to characterize, but we found that stiffer is not always better. The shortest practical length of tubing, based on mechanical constraints, is approximately 100 mm. While the larger ID tubing performed slightly better in terms of propagation velocity of the pressure wave, it suffered in rise time because of the large dead volume. The largest diameter tubing we tested (2.5 mm ID silicone) took more than 75 ms to reach steady state. Thin-walled tubing performed more poorly than thicker-walled, stiffer, tubing. Harder tubing such as Teflon produced pronounced ringing echos, and also coupled valve vibration into the pipette holder.

The best overall performance came from 100 mm, small ID (0.8 mm), thick-walled (4 mm OD), silicone tubing, which is shown in Fig. 7. If ringing in the propagated wave is ignored, the waveform at the end of the tube can be modeled as a simple exponential delay of the pressure wave measured at the valve:

$$P'_t = P'_{t-\mathrm{d}t} + \left(P_t - P'_{t-\mathrm{d}t}\right) \cdot \left(1 - e^{\frac{-\mathrm{d}t}{\tau}}\right) \quad (1)$$

where P_t and P'_t are the pressures at the valve and at the end of tubing, respectively, at time t. dt is the sample interval (100 µs) and τ the time constant. The data is first offset in time by 950 µs. Equation 1 is then applied recursively using a time constant of 448 µs. The time constant and time offset were determined empirically to give the best fit to the early part of the pressure waveform.

The system noise is shown in Fig. 8, and is dominated by turbulence from the air flow. When the pumps are off and there is no air flowing through the valve, the

Table 3 Effect of connecting tubing. Rise times are for a 40 mmHg step and are given as the 10–90% value. Delays are measured from the application of the pressure command step to the 10% pressure point. The delay from the headstage sensor to the valve outlet (no tubing) reflects the length of tubing used to connect the water detector. Tubing stiffness prevented use of PVC and Teflon in lengths shorter than 150 mm. All times are in milliseconds; all dimensions are in millimeters

Tubing type	Length	300 mm		150 mm		100 mm	
	I.D./O.D.	Delay	Rise time	Delay	Rise time	Delay	Rise time
Silicone	0.8/1.6	2.6	5.5	2.1	3.4	1.8	2.7
	0.8/4	2.4	4.0	1.8	2.1	1.6	1.7
	1.6/3.2	2.2	6.4	1.8	3.8	1.7	3.0
	2.5/4	2.3	12.8	1.9	7.1	1.7	4.8
PVC	0.8/1.6	2.4	3.7	1.9	2.5	–	–
	1.6/3.2	2.3	4.6	1.8	2.8	–	–
Teflon	1.4/1.9	2.4	5.8	1.9	3.7	–	–
No Tubing	N/A	1.4	1.2	–	–	–	–
Headstage	N/A	0.55	0.65	–	–	–	–

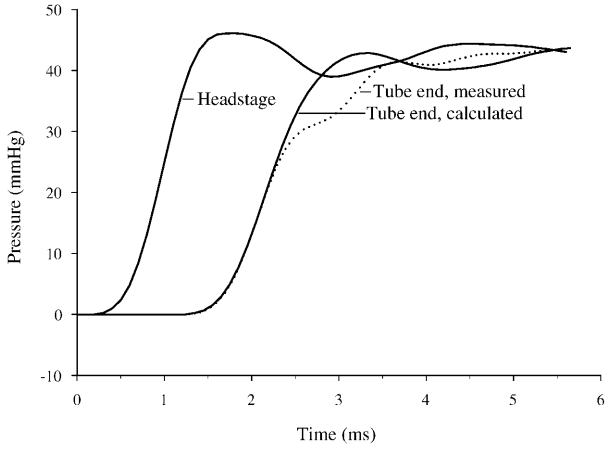

Fig. 7 Rise times with a 100 mm length of 0.8 mm ID/4 mm OD silicone rubber tubing. Time is measured from the application of the command pulse. The propagated pressure wave was modeled as a simple exponential delay with a time offset of 950 us and a time constant of 448 us. Reflections were not modeled

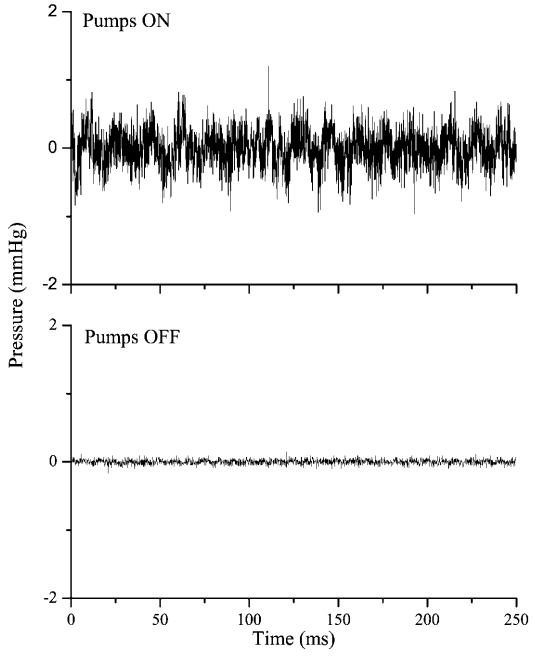

Fig. 8 System noise with pumps off (*lower panel*) or on (*upper panel*). The root mean square noise with the pumps on is 0.28 mmHg and with the pumps off, 0.04 mmHg

measured root mean square (RMS) pressure noise is 0.037 mmHg. Turning on the pumps increases the RMS noise to 0.28 mmHg. Power spectra of the excess noise is predominantly white with a significant component at 60 Hz from the pumps.

We have used the pressure clamp to measure the change in membrane capacitance resulting from stretching. Figure 9 shows a trace from an outside-out patch from astrocytes. The capacitance increased with pressure with a time constant <3 ms, a limit set by the lock-in

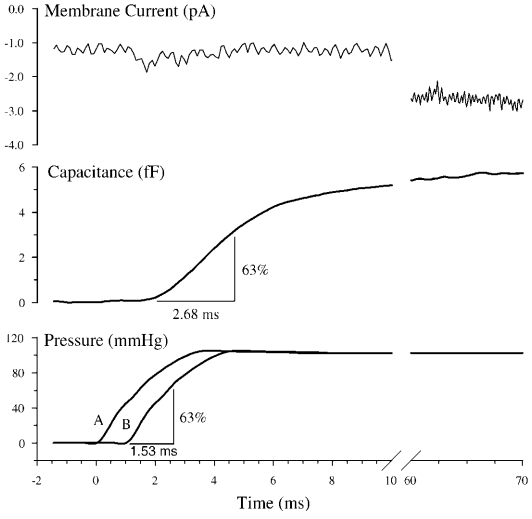

Fig. 9 Change in capacitance and channel current following a pressure step applied to an outside-out patch. The delayed pressure waveform was calculated as in Fig. 7. Rising phase time constants were estimated as (1–1/*e*) of the change in pressure or capacitance. Capacitance was measured at 8 kHz using a lock-in amplifier. Capacitance provides a measure of the local strain. The channels open with a substantial latency from the local strain

amplifier. After release of pressure, the capacitance fell with a similar time course. The response time of the pressure clamp at the patch was estimated using the same method used in Fig. 7 to calculate the tube-end pressure waveform and is also <3 ms. A trace of channel currents is included in Fig. 9 to illustrate that the mechanically gated response occurs milliseconds after the pressure and capacitance steps. This latency to the net stimulus would be missed without a fast pressure clamp.

Discussion

The new pressure clamp system has worked reliably in the laboratory in day-to-day experiments for 2 years [9]. The most straightforward improvement is the prevention of water entry. Since adding this feature to our pressure clamps, we have not had a single case of contamination. The new valve is also inherently more resistant to breakdown since the bimorph is electrically poled in parallel so that both the outer surfaces are kept at ground potential and only the center shim is driven. Furthermore, the center shim is only exposed to low voltages except during pressure changes and saturating drives. This is in contrast to the Lee valves, which are electrically poled in series. This requires that the outer surfaces of the piezo be held at a large static DC voltage (160–190 V), making the element subject to arcing and dielectric breakdown. Improvements in the valve response time have meant that the system response characteristics are stable over time.

The shorter valve activation latency permits the roll-off frequency of the feedback loop to be increased

without risk of destabilizing the servo. A 120-μs delay corresponds to a 180-degree phase shift at 4.2 kHz. As long as the feedback gain is less than 1 at this frequency, the latency is not a problem. The cause of the latency is not entirely clear, but is probably the result of several factors. Although the piezo element charges quickly, the mass of the piezo must be accelerated from rest and the pressure can't start changing until the piezo begins moving. A portion of the delay is due to the speed of sound. Traveling at 3.35 mm/μs (STP), the pressure wave will require about 24 μs. This is a conservative estimate since the speed of sound is reduced in the narrow gaps within the valve. It is unlikely that the effect of pressure on the speed of sound is a significant factor since the activation delay is the same on both the rising and falling phases of the response. Because the latency appears to be the result of several factors, it is not readily reduced.

The quest for speed of response is driven by the properties of mechanosensitive channels. Channel adaptation/inactivation occurs within 50–100 ms [1, 9] and the activation process is much faster. The speed of the present system is adequate for most studies of cell-attached and inside-out patch mechanics since those relaxation times are 10–500 ms [8]. However, as shown in Fig. 9, outside-out patches respond as fast as the clamp, and new technology will be required for higher time resolution.

Acknowledgements This work was supported by grants from the NIH to F.S. We would like to thank ALA Scientific (http://www.alascience.com/) for taking this design into production.

References

1. Hamill OP, McBride DW Jr (1992) Rapid adaptation of single mechanosensitive channels in *Xenopus* oocytes. Proc Natl Acad Sci USA 89:7462–7466
2. Hamill OP, McBride DW Jr (1995) Pressure/patch-clamp methods. In: Boulton A, Baker G, Walz W (eds) Neuromethods. Humana Press, Totowa, pp 75–87
3. McBride DW Jr, Hamill OP (1992) Pressure-clamp: a method for rapid step perturbation of mechanosensitive channels. Pflugers Arch 421:606–612
4. McBride DW Jr, Hamill OP (1993) Pressure-clamp technique for measurement of the relaxation kinetics of mechanosensitive channels. Trends Neurosci 16:341–345
5. McBride DW Jr, Hamill OP (1995) A fast pressure-clamp technique for studying mechanogated channels. In: Sakmann B, Neher E (eds) Single-channel recording. Plenum, New York, pp 329–340
6. McBride DW Jr, Hamill OP (1999) Simplified fast pressure-clamp technique for studying mechanically gated channels. Methods Enzymol 294:482–489
7. Sachs F (1987) Baroreceptor mechanisms at the cellular level. Fed Proc 46:12–16
8. Sokabe M, Sachs F, Jing Z (1991) Quantitative video microscopy of patch clamped membranes – stress, strain, capacitance and stretch channel activation. Biophys J 59:722–728
9. Suchyna TM, Johnson JH, Clemo HF, Huang ZH, Gage DA, Baumgarten CM, Sachs F (2000) Identification of a peptide toxin from *Grammostola spatulata* spider venom that blocks stretch activated channels. J Gen Physiol 115:583–598